JACS
JOURNAL OF THE AMERICAN CHEMICAL SOCIETY
Communication
pubs.acs.org/JACS

Single-Site Organozirconium Catalyst Embedded in a Metal−Organic Framework

Rachel C. Klet,[†] Samat Tussupbayev,[‡] Joshua Borycz,[‡] James R. Gallagher,[§] Madelyn M. Stalzer,[†] Jeffrey T. Miller,[§,∥] Laura Gagliardi,*[,‡] Joseph T. Hupp,*[,†] Tobin J. Marks,*[,†] Christopher J. Cramer,*[,‡] Massimiliano Delferro,*[,†] and Omar K. Farha*[,†,⊥]

[†]Department of Chemistry, Northwestern University, Evanston, Illinois 60208, United States
[‡]Department of Chemistry, Supercomputing Institute, and Chemical Theory Center, University of Minnesota, Minneapolis, Minnesota 55455, United States
[§]Chemical Sciences and Engineering Division, Argonne National Laboratory, Argonne, Illinois 60439, United States
[∥]School of Chemical Engineering, Purdue University, West Lafayette, Indiana 47907, United States
[⊥]Department of Chemistry, Faculty of Science, King Abdulaziz University, Jeddah, Saudi Arabia

Supporting Information

ABSTRACT: A structurally well-defined mesoporous Hf-based metal−organic framework (Hf-NU-1000) is employed as a well-defined scaffold for a highly electrophilic single-site d^0 Zr−benzyl catalytic center. This new material Hf-NU-1000-ZrBn is fully characterized by a variety of spectroscopic techniques and DFT computation. Hf-NU-1000-ZrBn is found to be a promising single-component catalyst (i.e., not requiring a catalyst/activator) for ethylene and stereoregular 1-hexene polymerization.

Heterogeneous catalysts have many attractions versus their homogeneous counterparts including recyclability, easy separation from product streams, and, often, greater thermal stability.[1] Nevertheless, despite their broad implementation, the design and synthesis of new highly active and selective heterogeneous catalysts remain a challenge. Typically, heterogeneous catalysts are supported on structurally/chemically irregular surfaces, rendering control of reaction selectivity and establishing structure−activity relationships challenging.[2] Such information is crucial for rational catalyst design, and precision methods are needed to prepare heterogeneous catalysts in a controlled, well-defined molecular manner and for their simultaneous computational characterization.

One strategy to access structurally well-defined heterogeneous catalysts is to employ atomically periodic scaffolds. The present approach utilizes a chemically and thermally robust metal−organic framework (MOF) in lieu of a traditional oxide/chalcogenide/nitride or activated carbon platform for supporting molecular complexes.[3] MOFs are three-dimensional, sterically/electronically tunable, crystalline, porous materials composed of inorganic nodes and organic linkers.[4] In contrast to the irregular surfaces of classical SiO_2 or Al_2O_3 supports, MOFs have inherently uniform surface structures.

Given the periodicity of MOFs, the potential to precisely determine atomic positions using single crystal X-ray diffraction, and reports of MOF-based catalytic selectivity,[5] we consider them promising and underexplored catalytic scaffolds. One class of MOFs that has gained attention for exceptional stability are Zr- and Hf-based MOFs,[6] such as NU-1000 (Zr) or Hf-NU-1000, which consist of Zr_6 or Hf_6 nodes $[M_6(\mu_3\text{-}O)_4(\mu_3\text{-}OH)_4(OH)_4(H_2O)_4$, M = Zr, Hf] and the tetra-carboxylate linker 1,3,6,8-tetrakis(*p*-benzoate)pyrene (H_4TBAPy).[5a,7] These MOFs have large 29−30 Å hexagonal mesopores that facilitate mass transport of both catalyst precursors and reactants/products, as well as accessible −OH and $-OH_2$ grafting sites, the topologies of which have been established by combined experimental and computational techniques.[9] The node −OH and $-OH_2$ sites are very acidic with the pK_a of the most acidic μ_3-OH proton ∼3.6.[10] Importantly, these protonolytic sites can be functionalized in many ways.[7,11]

To date, incorporation of catalytic metal centers into MOFs has followed three strategies: (1) inclusion into MOF pores,[12] (2) covalent attachment via organic linkers,[4d,5b] and (3) binding to inorganic node groups.[7,11a−c,13] Compared to inclusion complexes, node binding is more likely to afford stable and structurally precise catalysts.[14] Here we report the synthesis, characterization, and preliminary catalytic olefin polymerization properties of a single-component (i.e., not requiring a cocatalyst or activator), single-site, highly electrophilic d^0 organozirconium catalyst embedded in a well-defined Hf-NU-1000 scaffold (Scheme 1).

A benzene solution of tetrabenzylzirconium ($ZrBn_4$) was reacted with a benzene slurry of microcrystalline Hf-NU-1000 at 25 °C for 1 h in an Ar glovebox. The air-sensitive product was washed repeatedly with benzene to remove residual $ZrBn_4$, and the benzene supernatant exchanged with pentane to facilitate solvent removal from the functionalized MOF. The presence of Zr in Hf-NU-1000-ZrBn (Schemes 1B,C) was quantified with ICP−atomic emission spectroscopy. On average, 2.4 Zr atoms/Hf_6 node are incorporated (Table S1, SI)).[15] SEM−EDX indicates uniform Zr incorporation throughout the MOF crystallites (Figure S1).

The powder X-ray diffraction pattern (PXRD) of the Hf-NU-1000-ZrBn indicates that it retains crystallinity after ZrBn

Received: November 6, 2015
Published: December 14, 2015

DOI: 10.1021/jacs.5b11350
J. Am. Chem. Soc. 2015, 137, 15680−15683

Scheme 1. Synthesis of Supported Organozirconium Catalysts on (A) Silica,[8] (B) Hf-NU-1000, and (C) Schematic of Proposed Chemistry Creating Highly Electrophilic Zr Species on a MOF

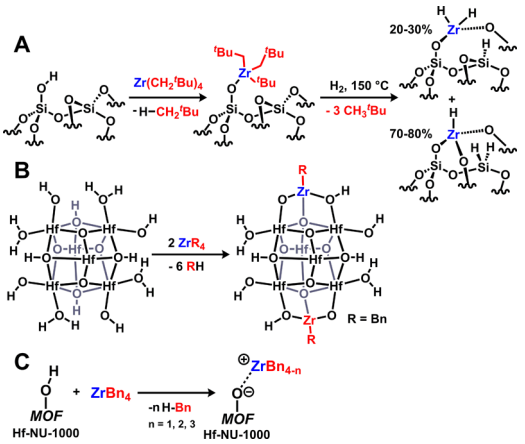

incorporation (Figure S3). Note also that N_2 adsorption isotherms for Hf-NU-1000-ZrBn reveal that, while the BET surface area decreases versus the parent Hf-NU-1000 material,[16] mesoporosity is maintained (Figure S4). Diffuse reflectance FT-IR spectroscopy of Hf-NU-1000-ZrBn confirms metalation via reaction with the node −OH and $-OH_2$ groups (Figure 1), evidenced by decreased intensity of the 3678 and 3679 cm^{-1} vibrational modes assigned to terminal −OH and $-OH_2$, respectively (Figure S2).

Next, the Hf-NU-1000-ZrBn structure was probed by solid-state ^{13}C CP−MAS NMR spectroscopy. The Hf-NU-1000-ZrBn spectrum exhibits aromatic resonances assignable to the carbon atoms of the framework TBAPy linkers, similar to the parent Hf-NU-1000 MOF;[17] however, the spectrum of Hf-NU-1000-ZrBn also exhibits a broad resonance centered at δ = ∼67 ppm, in the chemical shift range expected for a $Zr-CH_2$ carbon (Figure S6).[18] The ^1H MAS spectrum of Hf-NU-1000-ZrBn likewise reveals peaks at δ = 2.9 and 7.9 ppm, which are assignable to the $Zr-CH_2$ and $Zr-CH_2Ph$ protons, respectively (Figure S7).[19] These NMR data thus provide evidence for the presence of a $Zr-CH_2Ph$ moiety in Hf-NU-1000-ZrBn.

Additional information on the Hf-NU-1000-ZrBn structure is provided by X-ray absorption spectroscopy (XAS, Table S3). The XANES Zr K-edge energy of Hf-NU-1000-ZrBn is 18001.5 eV, very similar to that of ZrO_2 and consistent with a Zr(IV) formal oxidation state (Figure S9). The Hf-NU-1000-ZrBn EXAFS spectrum was fit by a difference method using reference compounds to determine the individual ligand scattering contributions (details in the SI).[20] The optimum fit around Zr was obtained with one Zr−Bn ligand and three Zr−O ligands. The derived Zr−C bond length is identical to that in $ZrBn_4$, 2.29 Å;[21] while the Zr−O bonds are slightly shorter than those in ZrO_2, 2.13 and 2.15 Å, respectively.[22]

Organozirconium precursor−MOF interactions were next modeled using DFT. Investigating the $ZrBn_4$ reaction with Hf-NU-1000 reveals that a Zr−monobenzyl species is the lowest energy product on the reaction pathway, with protonolytic release of the fourth and final benzyl ligand, yielding a purely Zr−oxo species, energetically unfavorable (see SI for details, Scheme S1, and Table S4). Zr species **C** of Figure 1 is thus predicted to be in the 4+ oxidation state and 4-coordinate with three "Hf−O" ligands, originating from the MOF Hf_6 node, and one benzyl ligand, likely coordinated η^2, in good agreement with the EXAFS and NMR data (Figure 1, middle, and SI). Furthermore, a second potential product is located, resulting from a carboxylate $-CO_2^-$ group (originating in the TBAPy linker) shifting from the Hf_6 cluster to the Zr of **C** to form species **C2**. **C2** can then react to eliminate toluene and form the product **D2** with no Zr−C bond (Scheme S2). **D2** is a four-coordinate Zr(IV) species with average Zr−O bond lengths of 1.99 Å (Figure 1, right, and SI).[23] While **D2** is determined to be ∼7 kcal/mol more stable than **C** and is the thermodynamic product of the $ZrBn_4$ reaction with Hf-NU-1000 (Table S4), the SS NMR spectroscopy, as well as catalytic results (*vide infra*), suggest that a significant fraction of MOF Zr centers are best represented by kinetic product **C**.

Zr−benzyl species are known catalysts for olefin polymerization, typically requiring a Brønsted or Lewis acid activator/cocatalyst to create coordinatively unsaturated electrophilic centers.[24] Addition of neat 1-hexene to Hf-NU-1000-ZrBn under Ar results in an immediate change of the solution viscosity, without activator/cocatalyst addition. After stirring for 1 h, the supernatant was decanted and the product polymer dried *in vacuo*. NMR spectroscopy of the resulting colorless highly viscous liquid reveals >95% *isotactic*-poly(1-hexene), consistent with a C_1-symmetric Zr catalytic center (Figures S16 and S17).[25,26] To the best of our knowledge, this is the first report of

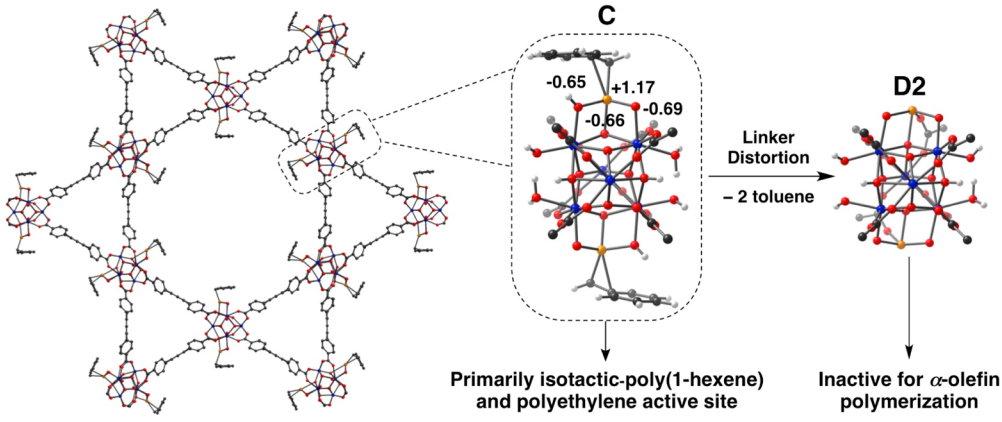

Figure 1. Calculated crystal structures showing a hexagonal pore of Hf-NU-1000-ZrBn with two Zr/Hf_6 clusters (left), close-up of Zr MOF component **C** with three Zr−O bonds and one Zr−Bn bond (middle), and close-up of Zr species **D2** with four Zr−O (right) and expected activities of **C** and **D2** with respect to ethylene and 1-hexene. Calculated CM5 charges are shown for Zr and the "Hf−O" ligands in species **C** (middle).

DOI: 10.1021/jacs.5b11350
J. Am. Chem. Soc. 2015, 137, 15680−15683

stereoregular polymerization by a MOF catalyst.[27] To obtain better insight into the origin of the regioselectivity, DFT calculations were performed to examine the insertion mechanism of an α-olefin into the Zr−Bn bond. At constant elevated [α-olefin], the turnover-limiting propagation/insertion step has a low computed barrier of ∼12 kcal/mol, with 1,2-insertion more favorable by ∼3 kcal/mol versus 2,1-insertion (Table S10). Note that no polymerization activity is observed upon 1-hexene addition to either the parent MOF Hf-NU-1000 or to solution phase $ZrBn_4$ under identical reaction conditions. Additionally, ICP analysis of the filtered reaction solution after catalysis indicates neither Zr nor Hf particles leached into the solution or into the polymer contained therein.

Furthermore, addition of 100 equiv of methylaluminoxane (MAO; 100 Al/Zr) to the 1-hexene before addition of the MOF-based catalyst yields no polymer.[28] Analysis of poly(1-hexene) by ^{1}H NMR indicates primarily vinylene end groups, consistent with a β-hydride elimination chain transfer pathway.[29] GPC reveals a bimodal mass distribution (M_n = 274 000 g/mol, PDI = 1.9 for the higher M_n fraction, and M_n = 570 g/mol, PDI = 1.2 for the lower M_n fraction), likely reflecting activity differences between interior and exterior MOF catalytic sites (Table S9).

The Hf-NU-1000-ZrBn 1-hexene polymerization activity is 1.4 × 10^2−2.4 × 10^3 g polymer (mol cat)$^{-1}$ h^{-1}; the lower range may reflect competitive formation of inactive species **D2** found in the DFT calculations (Figure 1). SEM and PXRD analysis of the MOF after polymerization (Figures S21 and S22, respectively) indicate that the MOF remains crystalline and that the crystallites are largely intact.[30] Notably, separation of the MOF catalyst from the poly(1-hexene) via filtration and addition of fresh 1-hexene monomer results in further polymerization activity (albeit with a lower activity: 1.2 × 10^2 g polymer (mol cat)$^{-1}$ h^{-1}). We expect that the lower activity for the second catalytic run likely results from incomplete separation of the polymer from the MOF, possibly blocking some active site pores. Nonetheless, this result indicates that Hf-NU-1000-ZrBn recyclability is promising.

Under the same catalytic conditions, Hf-NU-1000-ZrBn is also very active for ethylene homopolymerization (Table S9). Solution ^{13}C NMR spectroscopy of the product polymer reveals a single resonance at δ = 30 ppm typical of linear high-M_n polyethylene (Figure S24). The low polymer solubility precludes separation from the MOF for GPC analysis; however, DSC reveals a melting point (T_m) of 142 °C, suggesting ultrahigh-M_n polyethylene (Figure S25).[31] Hf-NU-1000-ZrBn activity for ethylene homopolymerization is 9.3 × 10^3 g polymer (mol cat)$^{-1}$ h^{-1}. The higher activity vs 1-hexene likely reflects MOF−Zr steric constraints. Attempts to copolymerize ethylene + 1-hexene under the same conditions result in negligible 1-hexene uptake, again likely reflecting the steric/kinetic constraints imposed by the MOF environment.

Hf-NU-1000-ZrBn single-site catalytic behavior without an activator/cocatalyst implies generation of a cationic/unsaturated Zr center. Indeed, the CM5 and natural population analysis (NPA) calculations on species **C** reveal substantial positive electron density at the Zr center and negative charge density on the surrounding O atoms (Figure 1, middle; Table S6), such that the Zr−MOF interaction is likely more ionic than covalent (Scheme 1C). This ionicity yields a highly electrophilic d^0 Zr center that enables monomer coordination, insertion, and propagation. In conclusion, a new, structurally well-defined, MOF-based cationic olefin polymerization catalyst was synthesized by incorporation of an organozirconium complex into Hf-NU-1000. Hf-NU-1000-ZrBn is an active single-component catalyst for ethylene and stereospecific 1-hexene homopolymerization.

■ ASSOCIATED CONTENT

Supporting Information

The Supporting Information is available free of charge on the ACS Publications website at DOI: 10.1021/jacs.5b11350.

General procedures, materials, and instrumentation; Hf-NU-1000-ZrBn synthesis and characterization, polymerization, and computational details (PDF)

■ AUTHOR INFORMATION

Corresponding Authors

*gagliardi@umn.edu
*j-hupp@northwestern.edu
*t-marks@northwestern.edu
*cramer@umn.edu
*m-delferro@northwestern.edu
*o-farha@northwestern.edu

Notes

The authors declare no competing financial interest.

■ ACKNOWLEDGMENTS

O.K.F., J.T.H., L.G., and C.J.C. acknowledge the financial support from the Inorganometallic Catalyst Design Center, an Energy Frontier Research Center funded by the U.S. DOE under award DE-SC0012702 (catalyst synthesis and characterization; computational modeling). M.D. and T.J.M. were supported by the Institute for Catalysis in Energy Processes (U.S. DOE) under award DE-FG02-03ER15457 (catalyst activity). This work made use of the EPIC facility (NU*ANCE* Center-Northwestern U.), which received support from the MRSEC program (NSF DMR-1121262) at the Materials Research Center; the International Institute for Nanotechnology (IIN); and the State of IL. Advanced Photon Source use was supported by the U.S. DOE, under award DE-AC02-06CH11357. MRCAT operations are supported by the U.S. DOE and the MRCAT member institutions. J.T.M. and J.R.G.'s funding was provided by the U.S. DOE under award DE-AC0-06CH11357.

■ REFERENCES

(1) de Jong, K. P. *Synthesis of Solid Catalysts*; Wiley-VCH: Germany, 2009.

(2) Thomas, J. M.; Thomas, W. J. *Principles and Practice of Heterogeneous Catalysis*; VCH: New York, 1997.

(3) For reviews of oxide-supported organometallic catalysts see: (a) Stalzer, M. M.; Delferro, M.; Marks, T. J. *Catal. Lett.* **2015**, *145*, 3. (b) Copéret, C.; Chabanas, M.; Saint-Arroman, R. P.; Basset, J. M. *Angew. Chem., Int. Ed.* **2003**, *42*, 156.

(4) (a) Furukawa, H.; Cordova, K. E.; O'Keeffe, M.; Yaghi, O. M. *Science* **2013**, *341*, 1230444. (b) Farha, O. K.; Hupp, J. T. *Acc. Chem. Res.* **2010**, *43*, 1166. (c) Horike, S.; Shimomura, S.; Kitagawa, S. *Nat. Chem.* **2009**, *1*, 695. (d) Lee, J.; Farha, O. K.; Roberts, J.; Scheidt, K. A.; Nguyen, S. T.; Hupp, J. T. *Chem. Soc. Rev.* **2009**, *38*, 1450.

(5) (a) Beyzavi, M. H.; Klet, R. C.; Tussupbayev, S.; Borycz, J.; Vermeulen, N. A.; Cramer, C. J.; Stoddart, J. F.; Hupp, J. T.; Farha, O. K. *J. Am. Chem. Soc.* **2014**, *136*, 15861. (b) Yoon, M.; Srirambalaji, R.; Kim, K. *Chem. Rev.* **2011**, *112*, 1196.

(6) (a) Furukawa, H.; Gándara, F.; Zhang, Y.-B.; Jiang, J.; Queen, W. L.; Hudson, M. R.; Yaghi, O. M. *J. Am. Chem. Soc.* **2014**, *136*, 4369. (b) Feng, D.; Gu, Z.-Y.; Li, J.-R.; Jiang, H.-L.; Wei, Z.; Zhou, H.-C. *Angew. Chem., Int. Ed.* **2012**, *51*, 10307. (c) Morris, W.; Volosskiy, B.; Demir, S.; Gándara, F.; McGrier, P. L.; Furukawa, H.; Cascio, D.; Stoddart, J. F.; Yaghi, O. M. *Inorg. Chem.* **2012**, *51*, 6443.

DOI: 10.1021/jacs.5b11350
J. Am. Chem. Soc. 2015, 137, 15680−15683

(7) Mondloch, J. E.; Bury, W.; Fairen-Jimenez, D.; Kwon, S.; DeMarco, E. J.; Weston, M. H.; Sarjeant, A. A.; Nguyen, S. T.; Stair, P. C.; Snurr, R. Q.; Farha, O. K.; Hupp, J. T. *J. Am. Chem. Soc.* **2013**, *135*, 10294.
(8) Basset, J.-M.; Copéret, C.; Soulivong, D.; Taoufik, M.; Cazat, J. T. *Acc. Chem. Res.* **2010**, *43*, 323.
(9) Planas, N.; Mondloch, J. E.; Tussupbayev, S.; Borycz, J.; Gagliardi, L.; Hupp, J. T.; Farha, O. K.; Cramer, C. J. *J. Phys. Chem. Lett.* **2014**, *5*, 3716.
(10) Klet, R. C.; Liu, Y.; Wang, T. C.; Hupp, J. T.; Farha, O. K. Unpublished, 2015.
(11) (a) Peters, A. W.; Li, Z.; Farha, O. K.; Hupp, J. T. *ACS Nano* **2015**, *9*, 8484. (b) Yang, D.; Odoh, S. O.; Wang, T. C.; Farha, O. K.; Hupp, J. T.; Cramer, C. J.; Gagliardi, L.; Gates, B. C. *J. Am. Chem. Soc.* **2015**, *137*, 7391. (c) Kim, I. S.; Borycz, J.; Platero-Prats, A. E.; Tussupbayev, S.; Wang, T. C.; Farha, O. K.; Hupp, J. T.; Gagliardi, L.; Chapman, K. W.; Cramer, C. J.; Martinson, A. B. F. *Chem. Mater.* **2015**, *27*, 4772. (d) Deria, P.; Bury, W.; Hupp, J. T.; Farha, O. K. *Chem. Commun.* **2014**, *50*, 1965.
(12) (a) Li, B.; Zhang, Y.; Ma, D.; Ma, T.; Shi, Z.; Ma, S. *J. Am. Chem. Soc.* **2014**, *136*, 1202. (b) Kalidindi, S. B.; Yusenko, K.; Fischer, R. A. *Chem. Commun.* **2011**, *47*, 8506. (c) Zhang, Z.; Zhang, L.; Wojtas, L.; Eddaoudi, M.; Zaworotko, M. J. *J. Am. Chem. Soc.* **2011**, *134*, 928.
(13) (a) Nguyen, H. G. T.; Schweitzer, N. M.; Chang, C.-Y.; Drake, T. L.; So, M. C.; Stair, P. C.; Farha, O. K.; Hupp, J. T.; Nguyen, S. T. *ACS Catal.* **2014**, *4*, 2496. (b) Meilikhov, M.; Yusenko, K.; Fischer, R. A. *J. Am. Chem. Soc.* **2009**, *131*, 9644.
(14) Node attachment is more likely to afford well-defined periodic species since installing appropriate grafting sites on linkers in a regular and controlled manner is often challenging.
(15) Longer exposure times or reaction at higher temperatures (50 °C) do not increase Zr incorporation (Table S1).
(16) This is consistent with what is observed by installing other metal ions in NU-1000; see refs 7 and 11a.
(17) Stylianou, K. C.; Heck, R.; Chong, S. Y.; Bacsa, J.; Jones, J. T. A.; Khimyak, Y. Z.; Bradshaw, D.; Rosseinsky, M. J. *J. Am. Chem. Soc.* **2010**, *132*, 4119.
(18) Popoff, N.; Macqueron, B.; Sayhoun, W.; Espinas, J.; Pelletier, J.; Boyron, O.; Boisson, C.; Merle, N.; Szeto, K. C.; Gauvin, R. M.; De Mallmann, A.; Taoufik, M. *Eur. J. Inorg. Chem.* **2014**, *2014*, 888.
(19) Such Zr−CH_2 protons are sensitive to environment and exhibit resonances over a broad range. The low Zr−CH_2 ^{13}C signal intensity precludes 2D $^{1}H-^{1}H$ DQMAS or 2D $^{1}H-^{13}C$ HETCOR NMR spectroscopy.
(20) Gu, W.; Stalzer, M. M.; Nicholas, C. P.; Bhattacharyya, A.; Motta, A.; Gallagher, J. R.; Zhang, G.; Miller, J. T.; Kobayashi, T.; Pruski, M.; Delferro, M.; Marks, T. J. *J. Am. Chem. Soc.* **2015**, *137*, 6770.
(21) Tedesco, C.; Immirzi, A.; Proto, A. *Acta Crystallogr., Sect. B: Struct. Sci.* **1998**, *54*, 431−437.
(22) Howard, C. J.; Hill, R. J.; Reichert, B. E. *Acta Crystallogr., Sect. B: Struct. Sci.* **1988**, *44*, 116.
(23) The EXAFS first shell data also fit model **D2** with four Zr−O bonds.
(24) Chen, E. Y.-X.; Marks, T. J. *Chem. Rev.* **2000**, *100*, 1391.
(25) Coates, G. W. *Chem. Rev.* **2000**, *100*, 1223.
(26) (a) Collette, J. W.; Tullock, C. W.; MacDonald, R. N.; Buck, W. H.; Su, A. C. L.; Harrell, J. R.; Mulhaupt, R.; Anderson, B. C. *Macromolecules* **1989**, *22*, 3851. (b) Yermakov, Y.; Zakharov, Y. *Adv. Catal.* **1975**, *24*, 173. (c) Ballard, D. G. H. *Adv. Catal.* **1973**, *23*, 263.
(27) (a) Madrahimov, S. T.; Gallagher, J. R.; Zhang, G.; Meinhart, Z.; Garibay, S. J.; Delferro, M.; Miller, J. T.; Farha, O. K.; Hupp, J. T.; Nguyen, S. T. *ACS Catal.* **2015**, *5*, 6713. (b) Li, H.; Xu, B.; He, J.; Liu, X.; Gao, W.; Mu, Y. *Chem. Commun.* **2015**, *51*, 16703.
(28) Babushkin, D. E.; Brintzinger, H.-H. *J. Am. Chem. Soc.* **2002**, *124*, 12869.
(29) Liu, S.; Motta, A.; Delferro, M.; Marks, T. J. *J. Am. Chem. Soc.* **2013**, *135*, 8830.
(30) MOF particles break up to some extent during the reaction due to mechanical stirring. See Figure S19 for a control reaction.
(31) Romano, D.; Andablo-Reyes, E.; Ronca, S.; Rastogi, S. *Polymer* **2015**, *74*, 76.

DOI: 10.1021/jacs.5b11350
J. Am. Chem. Soc. 2015, 137, 15680−15683